JACS
JOURNAL OF THE AMERICAN CHEMICAL SOCIETY

ARTICLE

pubs.acs.org/JACS

Three-Coordinate Ni^{II}: Tracing the Origin of an Unusual, Facile Si−C(sp^3) Bond Cleavage in $[(^tBu_2PCH_2SiMe_2)_2N]Ni^+$

Benjamin C. Fullmer, Hongjun Fan, Maren Pink, John C. Huffman, Nikolay P. Tsvetkov, and Kenneth G. Caulton*

Department of Chemistry, Indiana University, Bloomington, Indiana 47405, United States

Supporting Information

ABSTRACT: All attempts to synthesize (PNP)Ni(OTf) form instead ($^tBu_2PCH_2SiMe_2NSiMe_2OTf$)Ni($CH_2P^tBu_2$). Abstraction of F^- from (PNP)NiF by even a catalytic amount of BF_3 causes rearrangement of the (transient) $(PNP)Ni^+$ to analogous ring-opened $[(^tBu_2PCH_2SiMe_2NSiMe_2F)]Ni(CH_2P^tBu_2)$. Abstraction of Cl^- from (PNP)NiCl with $NaB(C_6H_3(CF_3)_2)_4$ in CH_2Cl_2 or C_6H_5F gives $(PNP)NiB(C_6H_3(CF_3)_2)_4$, the key intermediate in these reactions is $(PNP)Ni^+$, $[(PNP)Ni]^+$, in which one Si−C bond (together with N and two P) donates to Ni. This makes this Si−C bond subject to nucleophilic attack by F^-, triflate, and alkoxide/ether (from THF). This σ_{Si-C} complex binds CO in the time of mixing and also binds chloride, both at nickel. Evidence is offered of a "self-healing" process, where the broken Si−C bond can be reformed in an equilibrium process. $(PNP)Ni^+$ reacts rapidly with H_2 to give $(PN(H)P)NiH^+$, which can be deprotonated to form (PNP)NiH. A variety of nucleophilic attacks (and THF polymerization) on the coordinated Si−C bond are envisioned to occur perpendicular to the Si−C bond, based on the character of the LUMO of $(PNP)Ni^+$.

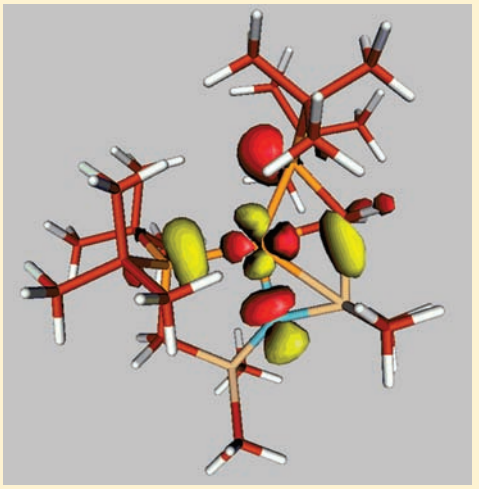

We were surprised to be able to synthesize[1] three T-shaped species (PNP)M, M = Fe, Co, and Ni, where PNP is the tridentate ligand $[(^tBu_2PCH_2SiMe_2)_2N]^-$[1], all of which have very low valence electron count. Much catalytic chemistry has been developed around such three-coordinate late transition metal species (or their synthons), including olefin polymerization and catalytic C−C bond formation between polar substrates.[2−11] Cationic three-coordinate species have been especially effective in this application and for olefin polymerization.[12−20] We wondered what reactivity changes would happen when we moved from d^8 (PNP)Co to the isoelectronic cation $(PNP)Ni^+$. In search of a precursor to such an electrophilic species, (PNP)$Ni(O_3SCF_3)$,[21,22] we found that halide metathesis from (PNP)NiCl with NaOTf (OTf = $F_3CSO_3^-$) or Me_3SiOTf was not successful. We therefore turned to an oxidative synthetic approach, the reaction of (PNP)Ni with AgO_3SCF_3. We report here the outcome of this reaction, which has led to the discovery of what we now establish to be *reversible* Si−C bond formation/scission in the unusual isolable species $(PNP)Ni^+$ (Scheme 1).

RESULTS

As mentioned in the introduction, preparation of (PNP)Ni(OTf) is not simple. Stirring of AgOTf with (PNP)NiCl for 2 days in THF shows essentially no conversion to the triflate[23] but only the production of increasing amounts of a silver phosphine complex, identifiable by its large $^{31}P\{^1H\}$ NMR doublet for each of the two silver isotopes (each I = 1/2).[24] We therefore tried a route beginning with monovalent, three-coordinate (PNP)Ni.

Redox Approach to "(PNP)Ni(OTf)". *1. Product Characterization.* The reaction of paramagnetic (PNP)Ni with equimolar AgOTf proceeds similarly in benzene and in THF with formation of a black solid (Ag^0). The phosphorus-containing material remains soluble; the $^{31}P\{^1H\}$ NMR spectrum, measured on material isolated after a reaction time of 12 h, shows an AX pattern with a large (82 ppm) difference in chemical shifts, and a $J_{PP'}$ large enough (213 Hz) to indicate *trans* phosphines in a single diamagnetic product. While the two P are inequivalent, there is a molecular mirror plane containing Ni, two P, and N since there are only two SiMe chemical shifts and two ^{t}Bu chemical shifts, the latter each being doublets (not virtual triplets). It is difficult to envision a structure that makes the two P inequivalent, but a single crystal structure determination of this compound, crystallized from pentane (Figure 1) reveals that there has been Si−CH_2 bond scission, and the silicon has captured the triflate as its new substituent. Triflate is not coordinated to the metal, but the resulting $^tBu_2PCH_2$ moiety is now bidentate on Ni^{II}. Despite their functional difference, the two phosphorus have essentially the same distance from Ni. The $^tBu_2PCH_2$ ligand (Scheme 2) can be thought of either as a

Received: September 17, 2010
Published: February 9, 2011

Scheme 1

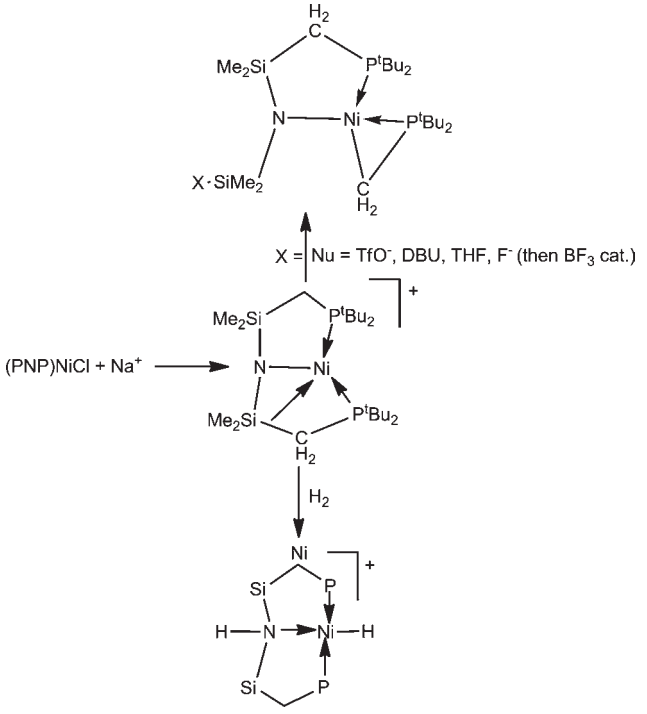

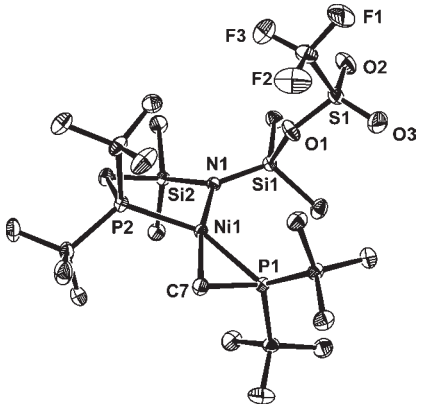

Figure 1. ORTEP view (50% probabilities) of the structure of [^{t}Bu$_2$PCH$_2$SiMe$_2$NSiMe$_2$(O$_3$SCF$_3$)]Ni[^{t}Bu$_2$PCH$_2$] with hydrogens omitted for clarity. Unlabeled atoms are carbons. Selected structural parameters: Ni−C7, 1.9598(14) Å; Ni−N1, 1.9784(11) Å; Ni−P1, 2.1933(4) Å; Ni−P2, 2.2018(4) Å; P1−C7, 1.7516(14)Å; C7−Ni−P2, 97.72(4)°; Ni−P1−C7, 58.30(5)°; Si1−O1−S1, 135.57(7)°; N1−Ni−P1, 49.74(3)°.

P-ylide with donation from the P=C bond and from a P−Ni σ bond or as a C-metalated phosphine accompanied by P lone pair donation; in either case the ligand is a 3-electron donor (neutral formalism) and the nickel is divalent. The nickel is rigorously planar and deviations from "square" planar are the angle N1−Ni−C7, which is 169.09(5)°, and also P1−Ni−P2, at 147.216(15)°. A ^{1}H NMR doublet with the unusual chemical shift of −0.5 ppm is assigned to the CH$_2$ protons of the ylide ligand.

2. Identification of an Intermediate. Earlier time observations (5 min after reagent mixing) of the solution ^{31}P NMR spectrum show that the reaction involves one detectable intermediate, having an AX ^{31}P{^{1}H} NMR pattern with very different

Scheme 2

Scheme 3

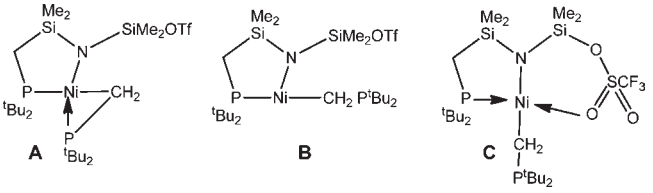

chemical shifts and a small (27 Hz) PP′ coupling constant. Over a period of hours in benzene, this species declines in intensity as signals of the crystallographically characterized product grow. One of the intermediate AX ^{31}P chemical shifts lies within 2 ppm of that for the final product (i.e., very similar environments in intermediate and final product), but the other lies 38 ppm downfield from the ^{t}Bu$_2$PCH$_2$ ligand of the final product. What is the intermediate on the way to the final product? Its ^{1}H NMR spectrum shows C_s symmetry, and the inequivalent phosphorus sites suggest that the Si−CH$_2$ cleavage has already occurred. We can account for the small PP′ coupling by avoiding having the two P mutually *trans*, but at least three structures qualify, all of which have the Si−O bond already formed (Scheme 3): **A** and **B** differ only in whether the Ni−P bond has been retained or broken. **A** is the least motion product, which keeps the CH$_2$ *cis* to the N it departed from. **B** is similar but is unusual in having Ni^{II} be only three-coordinate. **C** uses triflate to temporarily maintain coordination number 4 at Ni and awaits displacement of this O by the bulky ^{t}Bu$_2$P nucleophile. Both **A** and **B** have C_s symmetry, so this will not be a distinguishing feature of the observed ^{1}H NMR spectrum; **C** has no symmetry, due to the chiral sulfur, and is inconsistent with the molecular mirror symmetry indicated by the proton NMR. Why is the crystallographic product thermodynamically preferred to one of the suggested intermediate structures? The simplest explanation is that *trans* phosphines in Figure 1 minimize the mutual repulsion between four ^{t}Bu groups in **A**, which we suggest is the actual structure of the intermediate.

After a 12-h reaction time, the ratio of intermediate **A** to the crystallographic product is 1:9. Heating (60 °C) a pure (from selective crystallization) sample of the crystallographic product in benzene shows the reappearance of the intermediate, reaching relative populations of 1:9. This proves that the relative stability of the two is quite close and that the two are in equilibrium, even if they are connected by a significantly high barrier. All reactivity studies of (^{t}Bu$_2$PCH$_2$SiMe$_2$NSiMe$_2$OTf)Ni(CH$_2$P^{t}Bu$_2$) reported here are thus done with this 1:9 equilibrium mixture.

3. Mechanistic Generalities. Immediate observation of black silver metal implies that electron transfer is fast. To think of the detailed first mechanistic step, it may be that an adduct, (PNP)NiAgOTf, forms with a dative bond from dz^2 of Ni to Ag$^+$, and this collapses by inner sphere electron transfer to something where the contained atomic Ag^0 must now aggregate. Either of these species has an odd number of electrons so it would be ^{31}P NMR silent. However, we find that reaction of (PNP)Ni with equimolar [Cp*$_2$Fe]OTf in benzene gives results identical to those with silver triflate: both the intermediate and the final product are seen within 1 h of combining the reagents. Thus, any

dx.doi.org/10.1021/ja108426f |J. Am. Chem. Soc. 2011, 133, 2571–2582

Ag/Ni direct bonding is not uniquely responsible for the Si−C cleavage and the Si−O bond formation. Instead it occurs following outer sphere electron transfer, within a species of composition $(PNP)Ni^+$, partnered somehow with triflate.

Other Synthetic Approaches. We next carried out reactions designed to make authentic (PNP)NiOTf by a nonredox route: following synthesis of (PNP)NiF (see Experimental Section), this was reacted with equimolar Me_3SiOTf in benzene at 25 °C. There is a rapid color change, and NMR spectra recorded within 10 min of mixing show only the presence of the kinetic (i.e., P mutually cis, **A**) isomer $(^tBu_2PCH_2SiMe_2NSiMe_2OTf)Ni(CH_2P^tBu_2)$; after 3 h, the kinetic isomer and the crystallographic isomer are equally populated. This we believe indicates that either (PNP)NiOTf itself or the cation in any species $[(PNP)Ni^+][SiMe_3F(OTf)^-]$ is exceptionally reactive at the silicon of PNP, to permit triflate to attack as a nucleophile. Our belief that a cationic Ni species must be involved comes from the observation that (PNP)NiCl is recovered unchanged after 2 days in the presence of equimolar NaOTf in THF: free triflate does not attack Si in four-coordinate (PNP)NiCl.

Si−C Cleavage Mechanism. Why/how does this unusual reaction occur, to form a structure isomeric with the more conventional product, (PNP)Ni(OTf)? Why is this fundamentally rearranged species formed, and not simply (PNP)Ni(OTf)?[25−27]

We initially expected that the electrophilicity of $(PNP)Ni^+$ would have its influence on the N−Si bond. Although Si−O bond formation might have been anticipated, the fact that it happens with the weakly nucleophilic triflate is surprising. In close proximity to this $(PNP)Ni^+$ cation is triflate, which at least in benzene can be quite tightly ion paired (hence proximate for significant time) and also nucleophilic. It thus becomes capable of unusual triflate behavior, attack on Si. This still requires an explanation of selectivity of the bond cleaved: Si−N vs Si−C. Here selectivity is perhaps controlled by the potential for product stabilization: Si/N cleavage leaves nitrogen with a single substituent, which is oxidation (an imine, **D**), while Si−C cleavage leaves CH_2, which can be stabilized by binding to nickel. It is also relevant that, in $(PNP)Ni^+$, this is no ordinary CH_2, but one carrying an electrophilic substituent: four-coordinate phosphorus and thus analogous to a phosphonium cation. This stabilizes the evolving carbanion by ylide character.

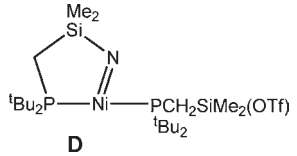

D

Toward Naked $(PNP)Ni^+$. Given our suspicion that cationic $(PNP)Ni^+$ might have exceptionally electrophilic character,[9,28−31] we sought to make this species in the absence of a nucleophilic anion. Reaction of (PNP)Ni with equimolar $[Cp^*_2Fe][B(C_6F_5)_4]$ in d_8-THF was carried out to evaluate the possibility of coordination of THF to $(PNP)Ni^+$. Reaction of (PNP)Ni with $[Cp^*_2Fe]BPh^F_4$ ($Ph^F = C_6F_5$) in THF immediately gives Cp^*_2Fe and a product with no $^{31}P\{^1H\}$ NMR signal, ruling out the formation of the adduct $(PNP)Ni(THF)^+$. The primary product first produced here (^{31}P NMR silent) is suggested to be $(PNP)NiBPh^F_4$. The ^1H NMR spectrum of this solution shows a doublet for ^tBu (hence not trans stereochemistry), one singlet for SiMe, and a broad (hence fluxional, near the decoalesence point) intensity 4 peak at −0.26 ppm attributed to the coalesced CH_2 groups. This negative chemical shift for the CH_2 protons is consistent with M/CH connectivity in an $M/C(sp^3)$ species[32−34] and shares that feature with $(^tBu_2PCH_2SiMe_2NSiMe_2OTf)Ni(CH_2P^tBu_2)$. Altogether, these indicate that an ether-free structure is preferred thermodynamically over coordination of THF. After 12 h at room temperature, this solution has transformed into a transparent glassy solid of polymeric THF.[35] The $^{31}P\{^1H\}$ NMR spectrum of this *sample* now shows narrow lines as an AX pattern with chemical shifts located within 4 ppm of those of $(^tBu_2PCH_2SiMe_2NSiMe_2OTf)Ni(CH_2P^tBu_2)$, consistent with cleavage of the ligand Si−C bond. The $J_{PP'}$ value, 198 Hz, is large enough to indicate trans positioning of these two nuclei. We suggest that the R group in the resulting $(^tBu_2PCH_2SiMe_2NSiMe_2OR)Ni(CH_2P^tBu_2)$ is the poly-THF chain. On the other hand, $(PNP)NiBAr^F_4$ survives for at least 6 days in CD_2Cl_2 solvent, so there is no chloride abstraction by this electrophilic nickel species.

Because of the polymerization of THF, we moved to more inert solvents (for a preliminary account, see ref 1). Reaction of (PNP)NiCl with 5-fold excess of $NaBAr^F_4$ in benzene (Ar^F = 3,5-$(CF_3)_2C_6H_3$) gives no change over 15 h; a polar solvent is needed. NMR of the product formed from this reaction in CD_2Cl_2 shows three proton chemical shifts but absolutely no $^{31}P\{^1H\}$ NMR signal at 25 °C. Since the proton chemical shifts were in the normal region, we felt that the absence of a phosphorus NMR signal was not due to paramagnetism. The $^{31}P\{^1H\}$ NMR spectrum recorded at −60 °C shows two equal intensity signals, each about 88 Hz wide at half height. At −40 °C these have each broadened significantly, indicating that the lack of ^{31}P NMR signal is due to room temperature being at the coalescence temperature. The room temperature ^1H NMR spectrum shows apparent C_{2v} symmetry (although the ^tBu signal is a doublet, not a virtual triplet), and only two aryl signals are seen (*ortho* and *para*), suggesting all four aryl rings are equivalent. Since one possible structure would have one pendant phosphine and achieve an 18-electron configuration by η^6 binding of one aryl ring, we looked at low temperature ^1H and ^{19}F NMR spectra in CD_2Cl_2. This showed no aryl region decoalescence by ^1H NMR and only a single signal by ^{19}F NMR. The mechanism of fluxionality leading to the coalescence at 25 °C was probed by adding $NaBAr^F_4$ to a CD_2Cl_2 solution of $(PNP)NiBAr^F_4$. This showed only one kind of aryl ring (*para* and *ortho* signals) and one signal for CF_3, indicating that free and any hypothetical "coordinated" BAr^F_4 are indistinguishable. Since the ^{19}F NMR spectrum did not decoalesce at −60 °C, and since the $^{31}P\{^1H\}$ NMR spectrum could be resolved to yield a $J_{PP'}$ value of 38 Hz at −55 °C, we abandoned the idea of coordinated arene and considered instead that both phosphorus are bound to Ni, but not in a *trans* stereochemistry. To establish additionally that the $(PNP)NiBAr^F_4$ product neither is paramagnetic nor has some cleavage of the PNP backbone, it was reacted with CO. This reaction went to completion in the time of mixing, to form a species whose characteristics are fully in agreement with C_{2v} symmetric $(PNP)Ni(CO)^+$, with a ν_{CO} value of 2044 cm^{-1}. Such a high ν_{CO} indicates high electrophilicity of the T-shaped $(PNP)Ni^+$ moiety.[36,37] Note that the 1-electron reduced species (PNP)Ni(CO) has a ν_{CO} of 1940 cm^{-1}.[38]

Solvent choice is essential to the synthesis of $(PNP)Ni^+$ from (PNP)NiCl. Whereas chloride is abstracted from (PNP)NiCl by $NaBAr^F_4$ in fluorobenzene or in dichloromethane, it is not in THF. Indeed $(PNP)Ni^+$ reacts with NaCl in THF to form

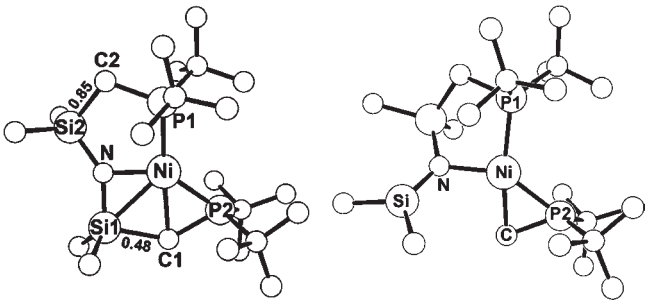

Figure 2. DFT geometry optimized structure of (left) $(PNP)Ni^+$, showing Mayer bond orders of two Si−C bonds, and (right) one bond-cleaved species. Hydrogens not shown.

(PNP)NiCl. This is apparently due to a combination of the higher solubility of NaCl in THF, as well as the fact that the electrophilicity of sodium in $NaBAr^F{}_4$ is diminished by coordination of THF to naked Na^+. If $[(PNP)Ni]BAr^F{}_4$ is synthesized from (PNP)NiCl and $NaBAr^F{}_4$ in CD_2Cl_2 and then separated by filtration from solid NaCl, and then the resulting $(PNP)Ni^+$ is dissolved in THF, the ^1H NMR signature of $(PNP)Ni^+$ is evident immediately after dissolution. At longer times, this THF solution of $(PNP)Ni^+$ shows polymerization of the THF to a solid but still narrow-line $^{31}P\{^1H\}$ NMR spectrum as an AX pattern with $J_{PP'}$ = 200 Hz. At shorter polymerization reaction observation times, the lines in the AX NMR pattern have multiple, closely spaced components, which we attribute to heterogeneity of molecular weights coming from varying polymer chain lengths attached to the pendant silyl group: $(^tBu_2PCH_2SiMe_2NSiMe_2OR^n)Ni(CH_2P^tBu_2)$, where R^n are these diverse polymer chain lengths.

An indication of the steric protection offered by the PNP ligand is available in that the SiMe ^1H NMR signals of a 1:1 mixture of $(PNP)Ni^+$ and (PNP)NiCl in CD_2Cl_2 shows separate resonances at 25 °C. Thus there is neither formation of a halide-bridged species nor exchange of the chloride between the two nickels, which is rapid on the ^1H NMR time scale.

Insight from DFT Energies and Structures. *1. Ground State Structure.* Survey of a variety of structures for $(PNP)Ni^+$ by DFT(PBE) calculations gave the surprising result that the global minimum singlet structure is Figure 2 (left). This has short distances from both Si1 (2.53 Å) and C1 (2.22 Å) to Ni; the metal satisfies its unsaturation by recruiting the Si−C bonding electron density as a donor. This is appropriately called a σ_{SiC} complex. In trying to understand how such an unconventional structure might be a minimum and be even more stable than the T-shaped alternative, we recognized that phosphorus in this structure has migrated and also reoriented its lone pair, to overlap better with the empty x^2-y^2 orbital that lies along the *y* axis (trans to N); in doing so, it pulls both Si and CH_2 closer to nickel, a donation from the Si−C bond to the lobe of the nickel x^2-y^2 directed along the *x* axis. Thus the phosphorus lone pair seeks out the best direction for overlap, not simply pointing toward the metal nucleus. Symptomatic of this orientation is that phosphorus is nearly coplanar with nickel and the two ^{t}Bu quaternary carbons. This C−Si distance has lengthened 0.16 Å compared to the other corresponding bond in this structure, and the Si−C1−P2 angle is large (135°). The angles Ni−P2−C(^{t}Bu) are all very large (122°), indicative of distortion of bonding at P2. Mayer bond orders are shown in Figure 2 and support the idea that short distances indeed involve partial chemical bond formation. In summary, the ground state structure of singlet $(PNP)Ni^+$ involves a highly activated Si−CH_2 bond (stretched to 2.07 Å), which is susceptible to attack even by a nucleophile as weak as triflate. This structure naturally explains the puzzling selectivity for cleavage of the Si−CH_2 bond rather than the Si−N bond. The nickel in $(PNP)Ni^+$ is thus highly electrophilic, which is the origin of the unusual ligand backbone coordination and cleavage; Si−C bond cleavage stabilizes a species with an activated Si−C bond and the Ni/C bond that must form upon Si−C bond scission is already attached to nickel. Attack (backside?) by X^- on this silicon will complete the formation of the primary product, $(^tBu_2PCH_2SiMe_2NSiMe_2X)Ni(CH_2P^tBu_2)$, detected by NMR spectroscopy. This transannular interaction of the Si−C bond with nickel has its precedents in agostic Si−C bonds,[39] as well as a transannular interaction in the olefin metathesis intermediate metallacycle $(R_3P)Cl_2RuCH_2CH_2CH_2$.[40]

2. T-Shaped and Si−C-Cleaved Alternatives. DFT(PBE) calculations on several other structures revealed some surprises. Three-coordinate T-shaped $(PNP)Ni^+$ is calculated to have a triplet state nearly degenerate with the singlet;[41] we have found that the higher spin state is very often favored in PNP species as a result of the low coordination number leaving numerous orbitals empty. Indeed, the normal ^1H NMR chemical shifts of $(PNP)Ni^+$ at 25 °C show that the triplet state is not responsible for the lack of ^{31}P NMR signal at 25 °C. The singlet here lies much closer to the ground state than it does for the isoelectronic cobalt analogue, Co(PNP), where the singlet lies 21 kcal/mol higher. Geometry optimization of the singlet species where the Si−CH_2 bond has been cleaved showed that this (Figure 2, right) is only 13.9 kcal/mol higher than the triplet three-coordinate species. The Ni−CH_2 bond has been fully formed in this species, and the interesting feature is how silicon responds to being three-coordinate. The silicon is coplanar with its three substituents and is eclipsed with the amide nitrogen plane and hence suitable for π overlap with the amide lone pair. In fact this Si−N bond length is 0.14 Å shorter than the other one in this structure, consistent with Si−N multiple bonding. Geometry optimization from a starting geometry where the $SiMe_2$ group of the Si−C cleaved product (Figure 2, right) is rotated 90°, to diminish such π bonding, minimizes to *reform* the Si−CH_2 bond, yielding the σ_{Si-C} complex[42−45] discussed above. A triplet state was also located for the Si−C cleaved species. It has a pseudotetrahedral coordination geometry, like classic four-coordinate Ni^{II} triplets, presumably because of occupancy of an x^2-y^2 orbital, which is strongly σ^* in a planar structure. However, its energy, +43.4 kcal/mol, makes it clear that the chemistry here must proceed further on the singlet surface.

X-ray Diffraction Structure Determination of $[(PNP)Ni]BAr^F{}_4$. The results and conclusions from this computational study of $(PNP)Ni^+$ were subsequently confirmed by an X-ray structure determination of the product from reaction of anhydrous $NaBAr^F{}_4$ with (PNP)NiCl in fluorobenzene solvent (Figure 3); once formed, this species can be dissolved without change in CH_2Cl_2, and it can be formed even with stoichiometric $NaBAr^F{}_4$. The X-ray result confirms the short contacts between Ni and CH_2 carbon and one Si and lengthening of that Si−C bond.[22,46−49] The unusual angles Ni−P−C(^{t}Bu) are also confirmed; the unconventional phosphorus has the *shorter* distance to nickel. The short contacts to Ni come at the expense of the unusual angle Ni−N1−Si1 = 89.3°, without distorting the H−C−H and Me−Si−Me angles at the unusual C and Si more than 5° from 109°. It is noteworthy that this Si−C bond donation is

dx.doi.org/10.1021/ja108426f |*J. Am. Chem. Soc.* 2011, 133, 2571–2582

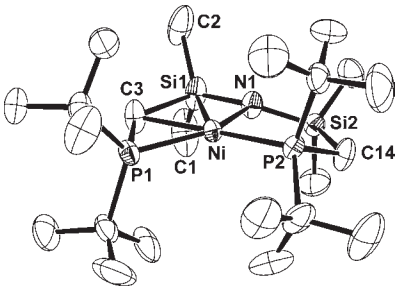

Figure 3. ORTEP view (50% probabilities) of the structure of $[(^tBu_2PCH_2SiMe_2)_2N]Ni^+$, from its $BAr^F{}_4$ salt, with hydrogens omitted for clarity. Unlabeled atoms are carbons. Selected structural parameters: Ni1−N1, 1.866(2) Å; Ni1−P1, 2.1201(8) Å; Ni1−P2, 2.189(6) Å; Ni−C3, 2.158(3) Å; Ni1−Si1, 2.494(2) Å; Ni−Si2, 3.135(1) Å; Si2−C14, 1.854(6) Å; Si1−C3, 2.069(4) Å; C3−P1, 1.840(3) Å; C14−P2, 1.818(17) Å; P1−Ni1−P2, 124.6(6)°; Si1−N1−Ni1, 89.27(13)°; Si2−N1−Ni1, 122.81(14)°; N1−Si1−C3, 103.92(16)°; P1−C3−Si1, 135.50(18)°.

energetically preferred to any C−H agostic donation or to ligand ^{t}Bu C−H cleavage, either heterolytic (H migrating to amide N) or oxidative addition to metal.

The phosphorus site exchange detected by ^{31}P NMR is then explained by reversing the roles of the two phosphine arms rapidly at room temperature via the T-shaped structure. We located a transition state between the σ_{Si-C} complex and the T-shaped (see Supporting Information), verified by one imaginary frequency, which is associated with motion along the Ni−C1 line. It lies above the σ_{Si-C} complex isomer by 11.9 kcal/mol, a magnitude that is consistent with the NMR coalescence. This TS is not the T-shaped species, since that is already verified to be a minimum. The misdirection of the P2 lone pair becomes evident with the loss of the Si−C donation since the Ni−P2 distance is longer (by 0.16 Å) than in either of the adjacent minima. On going to the TS from the σ_{Si-C} complex, the Ni−C1 distance is the most changed parameter, lengthened by 0.69 Å, with Ni−Si lengthened by 0.28 Å and C1−Si shortened by 0.12 Å. At the TS, ∠P1−Ni−P2 has increased by 28°, and ∠Ni−N−Si1 has increased by 13.6°. The small $J_{PP'}$ value in the decoalesced spectrum is due to these two nuclei being much less than 180° apart.

The LUMO of the σ_{Si-C} complex (Figure 4) shows that orbital has Si−C participation; however, this is not on the back side of silicon but is instead along the Si−C internuclear line, and thus, as observed experimentally, a nucleophile (triflate or fluoride or THF) will attack perpendicular to that bond, not at the back side of the silicon, *anti* to the Si−C bond.

BF_3 Catalysis of Si−C Cleavage. We wanted to probe the hypothesis that even a weaker nucleophile could cleave the stretched Si−C bond of naked $(PNP)Ni^+$. One approach to this would be to use a Lewis acid to abstract fluoride from (PNP)NiF. If the Lewis acid would then shuttle fluoride to silicon and cleave the ligand Si−C bond, the Lewis acid would be regenerated (Scheme 4), making the rearrangement/isomerization catalytic in Lewis acid. We chose $BF_3\cdot OEt_2$ for this purpose. Indeed, in time of mixing at 25 °C in benzene, 30 mol % $BF_3\cdot OEt_2$ converts (PNP)NiF completely into two molecules (9:1 mol ratio), each with a $^{31}P\{^1H\}$ NMR spectrum that is an AX pattern with additional splitting due to ^{19}F. Both products show a $J_{PP'}$ value large enough to qualify as having transoid location of the phosphorus nuclei. Given the product ratio and the lack of a signal for $BF_3\cdot OEt_2$ in the ^{19}F NMR of the product,

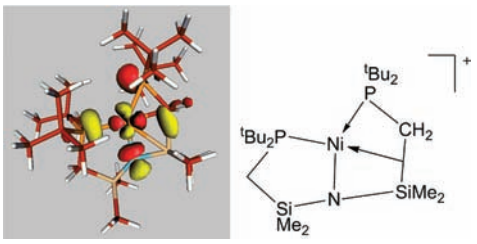

Figure 4. LUMO of the σ_{Si-C} structure found for $(PNP)Ni^+$.

we suspected that the two products were $[(^tBu_2PCH_2SiMe_2NSiMe_2F)]Ni(CH_2P^tBu_2)]$ and its adduct with the available BF_3 attached to the SiF fluorine. The fluorine NMR spectrum of the product solution shows one broadened quartet, assigned to the BF_3 on SiF, one broadened F at 1/3 the intensity, assigned to that Si−F, and (at higher intensity) one sharp doublet of multiplets, assigned to the fluorine in boron-free $[(^tBu_2PCH_2SiMe_2NSiMe_2F)]Ni(CH_2P^tBu_2)$; the doublet splitting is due to P, and the smaller splitting is due to the 6 protons of the near $SiMe_2$ group. Indeed this SiMe is a doublet in its ^{1}H NMR spectrum with the same J value (6 Hz) found in the ^{19}F NMR spectrum. The fact that the fluorine and ^{31}P and ^{1}H NMR spectra of this mixture show separate resonances for $[(^tBu_2PCH_2SiMe_2NSiMe_2F)]Ni(CH_2P^tBu_2)]$ and its BF_3 adduct means that any migration of BF_3 to a different Si−F is slow on the NMR time scale; this is supported by the fact that P−F coupling is retained (i.e., spin correlation persists) in the signal of one of the two phosphorus nuclei in the BF_3 adduct. The ESI+ mass spectrum of this sample, dissolved in THF, shows a molecular ion for protonated $[(^tBu_2PCH_2SiMe_2NSiMe_2F)]Ni(CH_2P^tBu_2)$, with the nickel isotope pattern but a stronger peak for protonated $[(^tBu_2PCH_2SiMe_2NH)]Ni(CH_2P^tBu_2)$, a species where the $SiMe_2F$ group has been removed and replaced by one proton. While the BF_3 adduct discussed above does not survive ESI-MS injection conditions in this THF solution, the identity of this more abundant N/Si-cleaved ion is supported by crystals formed in a reaction of *equimolar* (PNP)NiF and $BF_3\cdot OEt_2$.

A single crystal X-ray structure determination of this product shows (Figure 5) that the silyl group has been lost, probably as $SiMe_2F_2$, and the amide nitrogen has been doubly protonated, hence the compound is the BF_4 salt $[(^tBu_2PCH_2SiMe_2NH_2)]Ni(CH_2P^tBu_2)BF_4$. This is the 1:2 product of reaction of $(PNP)Ni^+$ with adventitious HF in the available $BF_3\cdot OEt_2$. The structure of this molecule shows it to be a hydrogen-bonded pair, with one fluorine hydrogen-bonded to one NH_2 proton. The second NH_2 proton hydrogen bonds to a different symmetry-related BF_4, and thus both F2 and F4 are involved in hydrogen bonding in a chain motif. The B−F distances to each of these two fluorines is longer by 0.024 Å (2.4 σ) and 0.039 Å (3.9 σ) than to the other two uninvolved F. The two phosphorus nuclei are located trans. Nickel is coplanar with its attached P1, P2, N1, and C12 (angles sum to 359.98°). The P2−C12 distance in the $^tBu_2PCH_2$ ligand is shorter than that in the five-membered ring, and the P2−Ni distance is shorter than that in the five-membered ring.

DFT(PBE) calculations on the species in Scheme 4 show that BF_4^- coordinates to $(PNP)Ni^+$, so separated ions are unnecessary for the catalyzed fluoride transfer mechanism. The DFT geometry optimization shows that the final product adduct with BF_3 is calculated to be more stable, by 17.2 kcal/mol in free energy, when the BF_3 binds to the amide nitrogen (Figure 6a),

dx.doi.org/10.1021/ja108426f |*J. Am. Chem. Soc.* 2011, 133, 2571–2582

Scheme 4. BF_3 Catalysis of F Migration, Showing Reaction Energies (kcal/mol)

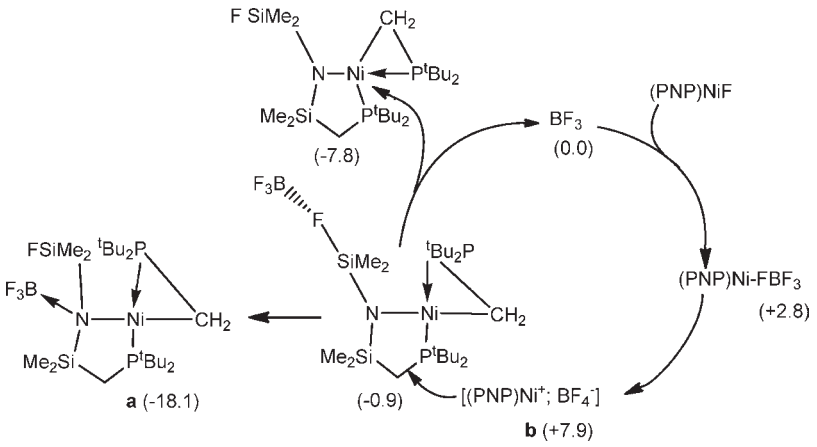

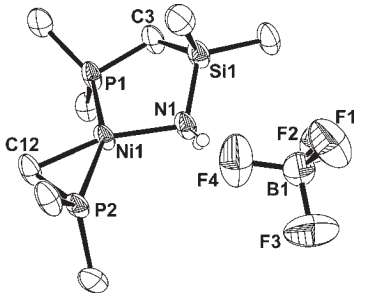

Figure 5. ORTEP view (50% probabilities) of the structure of $[^tBu_2PCH_2SiMe_2NH_2(BF_4)]Ni[^tBu_2PCH_2]$ with hydrogens and ^{t}Bu methyls omitted for clarity. Unlabeled atoms are carbons. Selected structural parameters: Ni1—C12, 1.956(5) Å; Ni1—N1, 1.992(4) Å; Ni1—P2, 2.1466(14) Å; Ni1—P1, 2.2272(15) Å; B1—F1, 1.359(9) Å; B1—F3, 1.360(9) Å; B1—F4, 1.383(9) Å; B1—F2, 1.399(8) Å; Si1—N1, 1.772(5) Å; C12—P2, 1.741(6) Å; C3—P1, 1.833(5) Å; C12—Ni1—N1, 162.0(2)°; C12—Ni1—P2, 49.95(16)°; N1—Ni1—P2, 112.33(13)°; C12—Ni1—P1, 104.49(17)°; N1—Ni1—P1, 93.21(13)°; P2—Ni1—P1, 154.44(6)°.

rather than to the fluorine of the Si—F group (Scheme 4); such a structure could also be in accord with our spectroscopic data. The lesser thermodynamic stability of BF_3 on F than on N is reflected in the structural parameters of each calculated structure (see Supporting Information). Boron is much less pyramidal when it is attached to F on Si than when it is on N, and the B—F(Si) distance is longer than the other three (terminal) B—F distances by 0.49 Å. We found a stationary state (Figure 6b) that is an ion pair between BF_4^- and the σ_{Si-C} complex geometry of (PNP)Ni^+, with the BF_4^- lying above the coordination plane and hydrogen-bonded to a number of aliphatic hydrogens, as well as interacting with nickel by one fluorine; this structure is an attractive intermediate for delivery of fluorine to silicon in nonpolar benzene. Note the σ_{Si-C} complexation already evident in this structure.

Reaction of ($^tBu_2PCH_2SiMe_2NSiMe_2OTf$)Ni($CH_2P^tBu_2$) with H_2. We next investigated how the Ni-CH_2 bond of ($^tBu_2PCH_2SiMe_2NSiMe_2OTf$)Ni($CH_2P^tBu_2$) might react with H_2.

1. Product Characterization. ($^tBu_2PCH_2SiMe_2NSiMe_2OTf$)Ni($CH_2P^tBu_2$) in benzene reacts slowly under 1 atm of H_2, with the reaction essentially complete within 7 days at 25 °C. The product, (PN(H)P)NiH^+, exhibits a hydride triplet, and the triflate salt slowly precipitates from the reaction solution as pale yellow needles. The product formed has C_s symmetry from its proton and phosphorus NMR spectra (the latter a doublet with selective hydride coupling, establishing the presence of a single hydride), which indicates the surprising *reformation* of a pincer ligand by Si—C coupling. The ^{1}H NMR spectrum of this isolated solid, dissolved in THF, shows a broadened intensity 1 signal at 2.9 ppm, which we attribute to formation of an amine still coordinated to nickel (Scheme 5).

The structure of [(PN(H)P)NiH]OTf was established by a single crystal X-ray diffraction study. While a fully satisfactory refinement model could not be found (see Supporting Information), the connectivity was established and shows a planar four-coordinate (PN(H)P)NiH^+ moiety, with triflate hydrogen-bonded to the amine proton. The overall idealized symmetry is C_s, consistent with the spectroscopic data.

2. Mechanistic Studies. The reassembly of the cleaved ligand is surprising on multiple counts. Apparently carbon of the CH_2-P^tBu_2 ligand is nucleophilic, retaining an ability to attack the silicon carrying the good leaving group triflate. Support for this comes from our ability to establish that it is the (less populated) isomer with this carbon *cis* to the pendant silyl group that disappears faster under H_2, detectable since the equilibrium between the two isomers is slower than the reaction of the *cis* isomer with H_2. The reaction is heterolytic splitting of H_2, made possible in part by the Bronsted basic amide nitrogen. Conventional wisdom certainly would have this happening from an H_2 complex, since these are known to be Bronsted acidic. If such an Ni(H_2) intermediate protonates nitrogen, the resulting reduced amide/silicon donation may make four-coordinate silicon become quite electrophilic and hence subject to attack by even a weak carbon nucleophile. Recall also that the triflate-loss species (Figure 2, right), where the $SiMe_2$ plane is perpendicular to the NiP_2N plane, is not a stationary state but collapses to form a bond between that Si and the ylidic CH_2 carbon; thus any removal of triflate from that silicon plausibly leads it to seek out the electron density of that carbon. Once formed, an NH group could hydrogen bond to neighboring silyl triflate, enhancing its leaving group character. We suggest that hydrogenolysis of the Ni—CH_2 bond of ($^tBu_2PCH_2SiMe_2NSiMe_2OTf$)Ni($CH_2P^tBu_2$)

dx.doi.org/10.1021/ja108426f |*J. Am. Chem. Soc.* 2011, 133, 2571–2582

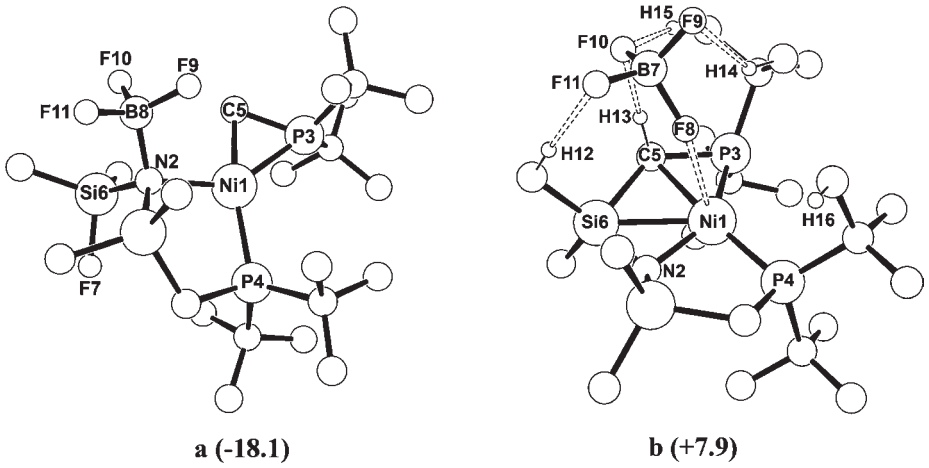

Figure 6. DFT geometry-optimized structures and energies (kcal/mol) of species relevant to Scheme 4.

Scheme 5

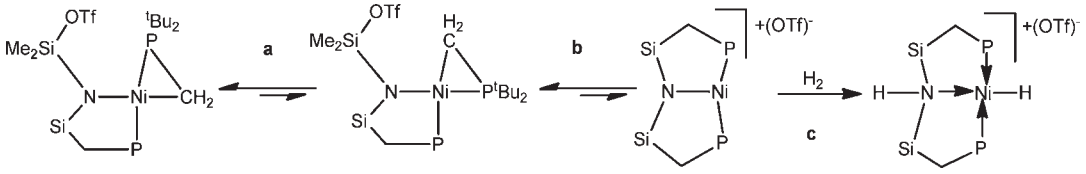

never occurs during the observed reaction, since once formed, a $^{t}Bu_2PMe$ ligand should survive unaltered.

How can this ligand reassembly be "triggered" by H_2? We suggest (Scheme 5) that the Si−C bond formation happens independent of the H_2 and that the role of H_2 is simply to trap the reassembled isomeric form. That is, we propose that the Si−C cleaved neutral species is in spectroscopically undetectable equilibrium with authentic $(PNP)Ni^+$ (**b**, Scheme 5). The observations establish that it is the *cis* isomer that reacts fast with H_2 and that the *trans* isomer only slowly disappears as a result of its slower rate of isomerization to the *cis* form (**a**, Scheme 5). Thus the species in the rapid but endergonic equilibrium with $(PNP)Ni^+$ is the *cis* isomer, where Si is proximate to the CH_2. The reassembly to form $(PNP)Ni^+$ is thus a reaction where triflate finally shows its leaving group character, since its departure from silicon is responsible for reforming the Si−C bond in the reversible equilibrium that is shifted by H_2. It is also true, since $(^{t}Bu_2PCH_2SiMe_2NSiMe_2OTf)Ni(CH_2P^{t}Bu_2)$ slowly polymerizes THF, that this supports the presence of a trace equilibrium amount of $(PNP)Ni^+$.

Deprotonation of (PN(H)P)NiH$^+$. To test the hypothesis in **c**, Scheme 5, reaction of $[(PNP)Ni]BAr^F{}_4$ with 1 atm of H_2 in CH_2Cl_2 was observed to occur rapidly, to form the $BAr^F{}_4$ salt of the same cation discussed above, $(PN(H)P)NiH^+$. In its reaction with H_2, $(PNP)Ni^+$ thus shows addition of nucleophilic H^- to nickel, not to the Si−C bond. This cation was deprotonated rapidly by $LiN^{i}Pr_2$ in THF to give the neutral (PNP)NiH. While this heterolytic splitting of H_2 (vs oxidative addition) is to be expected (Scheme 5c) on divalent nickel, it gets an assist from the Bronsted basic character of the amide nitrogen. With this now established as a rapid reaction of the intact $(PNP)Ni^+$ species, this becomes attractive not only as the thermodynamic driving force for the slow reaction of H_2 with $(^{t}Bu_2PCH_2SiMe_2NSiMe_2OTf)Ni(CH_2P^{t}Bu_2)$ but also for the mechanism described above. The slow rate of that reaction is then attributed to the difficulty of removing triflate from silicon in **b**, Scheme 5. This may be slowly initiated by acidic impurities, including the glass surface, but then might become autocatalytic once some of the acid [(PN(H)P)NiH]OTf is formed.

To try to carry out a one-pot conversion of $(PNP)Ni^+$ with H_2 and base to give (PNP)NiH, we also employed a base often considered[50] to be proton-specific, DBU (Scheme 6). In a preliminary control experiment, addition of DBU to a CD_2Cl_2 solution of $[(PNP)Ni^+]BAr^F{}_4$ in a 1:1 mol ratio gives immediate conversion to a species with an AX $^{31}P\{^1H\}$ NMR spectrum, with a $J_{PP'}$ = 30 Hz, indicative of the two P being *cis* in a species like that of $(^{t}Bu_2PCH_2SiMe_2NSiMe_2X)Ni(CH_2P^{t}Bu_2)$ where X = triflate (Scheme 6). Remarkably, this indicates that DBU functions as a nucleophile, binding to one silicon to give an iminium substituent on that arm of backbone-cleaved PNP ligand. This solution evolves, with a half-life of ∼12 h, with growth of a new AX $^{31}P\{^1H\}$ NMR pattern with the large $J_{PP'}$ (205 Hz) consistent with the two phosphorus nuclei mutually *trans*, thus indicating *trans*-$(^{t}Bu_2PCH_2SiMe_2NSiMe_2DBU)Ni(CH_2P^{t}Bu_2)^+$. Each isomer has spectra in agreement with C_s symmetry, thus two ^{t}Bu doublets and two SiMe singlets, together with a doublet for each isomer at negative chemical shifts, characteristic of a CH_2PR_2 ligand. If this mixture of *cis*- and *trans*-$(^{t}Bu_2PCH_2SiMe_2NSiMe_2DBU)Ni(CH_2P^{t}Bu_2)^+$ is subjected to 1 atm of H_2 there is slow (9 d) disappearance of both isomeric cations to form a mixture of (PNP)NiH and $(PN(H)P)NiH^+$. This hydrogenolysis reaction is much slower than that of $(PNP)Ni^+$ with H_2, suggesting that there is an equilibrium as in Scheme 5 and that the excess DBU present shifts the equilibrium away from $(PNP)Ni^+$, hence slowing the overall conversion. For comparison, equimolar NEt_3 fails to deprotonate $(PN(H)P)NiH^+$ in an attempted one-pot synthesis from $(PNP)Ni^+$ and NEt_3 under H_2; this also shows that NEt_3 fails to attack the

dx.doi.org/10.1021/ja108426f |*J. Am. Chem. Soc.* 2011, 133, 2571–2582

Scheme 6

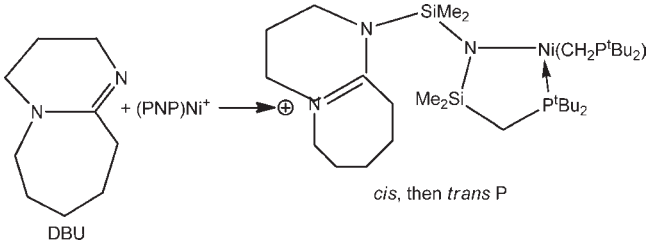

silicon of $(PNP)Ni^+$. A 10-fold excess of NEt_3 gives only 90% deprotonation.

DISCUSSION

We report four related $(^tBu_2PCH_2SiMe_2NSiMe_2X)Ni(CH_2P^tBu_2)$ species here, with X = F, OTf, O-polymer, and FBF_3. The difference in ^{31}P chemical shifts in a given species varies by only 7 ppm among these, and $J_{PP'}$ varies by 50 Hz, or 20%. The homology of these species is thus clear.

The pincer backbone bond cleavage described here shows a vulnerability of the ligand, particularly the Si−C bond, to nucleophilic attack. This redirects use of *this* electrophilic pincer complex to non-nucleophilic reaction conditions; H_2 is one example. At the same time, the reformation of this bond in Scheme 5, reaction **b** shows a remarkable thermodynamic proximity of the intact pincer; this equilibrium represents an unusual "self-healing" behavior which decreases the vulnerability to pincer backbone damage.

Consistent with the idea that this Si−C cleavage reaction derives from the electrophilicity of the N−Ni unit as a whole, we have previously observed Si−C bond cleavage,[51] forming **E**, where the oxidant (eq 1) was ferricinium cation and the trapping nucleophile was intramolecular (nitride). This can now be seen as $(PNP)CoN^+$ trapping electrophilic silicon with nitride, as well as with phosphorus. In brief, d^4 singlet $(PNP)CoN^+$ is a candidate for σ_{Si-C} complexation, which can trigger cleavage of that bond.

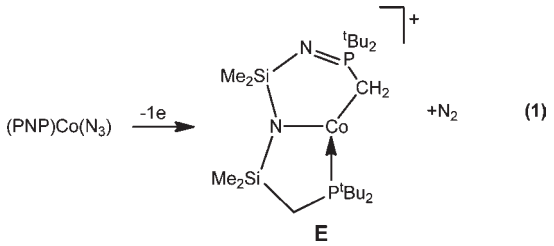

(1)

E

Since 3d metals are harder to oxidize than their heavier group analogues, this is an additional reason why some of the oxidation occurs at the nickel pincer amide N in contrast to 4d and 5d analogues; that is, the HOMO of the oxidized material has greater amide participation for the 3d case. To the extent that the nitrogen is partially oxidized, it becomes a poor leaving group. This contributes to selectivity for Si−C, not N−C, bond rupture.

Broadened Consideration of σ_{SiC} Complexation. A key question is the generality of this unusual phenomenon of Si−C σ complexation. We have probed this with DFT(PBE) calculations on some relevant comparison cases (Figures 7, 8, and 9, where all cases are on the same energy scale; see also Supporting Information). The several isomer energies are very densely packed for nickel. Calculations (Figure 7) show that, beyond what we considered earlier,[51] isoelectronic but lower valent (PNP)Co does indeed have a σ_{SiC} complex as a minimum, lower in energy than the T-shaped singlet by 7.5 kcal/mol. It is also lower than the oxidatively added species (PNP*)CoH by 2.5 kcal/mol. However it is *higher* in energy than triplet T-shaped (PNP)Co by 15.7 kcal/mol, consistent with the fact that this is the observed structure. Moreover, the (at least half) occupancy of all d orbitals in the triplet state makes the σ_{Si-C} structure implausible. In general, one needs to consider other factors for Si−C coordination: the x^2-y^2 orbital must be empty (singly occupied is not sufficient), the metal must be in an oxidation state with satisfactory energy match between a d orbital and the σ_{Si-C} bond orbital (i.e., the metal must be very electron-poor or electrophilic), and the energy of the intramolecular C−H cleavage isomer must be higher. Thus, going to more electron-rich rhodium (Figure 8), the singlet T-shaped structure is 6.7 kcal/mol more stable that the triplet (due probably to larger d-orbital splitting moving down a group) but the σ_{Si-C} structure is higher in energy (but by a negligible 0.90 kcal/mol) than (PNP*)RhH; this last structure is what is found experimentally. We therefore speculate as follows. This effect of larger d orbital splitting destabilizing the triplet state energy may favor the σ complexation for $(PNP)M^+$ where M is Pd or Pt, if C−H oxidative addition is still less stable there. d^8 $(PNP)Au^{2+}$ is even more likely to adopt a σ_{Si-C} structure. The d^6 configuration is another way to leave x^2-y^2 empty, but our calculations (Figure 9) show that the preference for low-coordinate 3d species to be high spin trumps the σ_{Si-C} structure. Thus, although the σ_{Si-C} complex isomer is competitive with various singlet and triplet Fe^{2+} structures, quintet T-shaped $(PNP)Fe^+$ is most stable of all, so the orbital half-occupancy in this structure precludes any σ_{Si-C} complex being the ground state. Consistent with the lowest reducing power of the 3d metal, the C−H oxidatively added isomer is never energetically competitive. The d^6 species Ru^{2+} shows the quintet to be least stable, due to the large d orbital splitting, but here the oxidatively added singlet is the global minimum. Experimentally, for d^6 $(PNP)Ru(N_2)(OTf)$, *heterolytic* splitting of an H−C(sp^3) bond[52] dominates over Si−C cleavage. The σ_{Si-C} structure of $(PNP)Ru^+$ is competitive for both singlet and triplet but is not the ground state. As is evident from all these calculations, the best general conclusion is that these late metal, high d electron count $(PNP)M^{q+}$ species have a great variety of redox and geometric isomeric structures at competitively *similar* energies, especially given the errors involved in the calculations.

EXPERIMENTAL SECTION

All reactions were performed in an argon glovebox or on a Schlenk line using standard air-sensitive techniques. Solvent distillation was carried out using either Na/benzophenone, CaH_2, 4 Å molecular sieves, a Grubbs-type purification system, or a combination of the four. Solvents were degassed and stored in airtight glassware. $[(^tBu_2PCH_2SiMe_2)_2N]Ni$ was prepared following the published[38] synthesis. ^1H NMR chemical shifts are reported in ppm relative to protio impurities in the deuterated solvents. $^{31}P\{^1H\}$ spectra are referenced to external standards of 85% H_3PO_4 (at 0 ppm). NMR spectra were recorded with a Varian Gemini 2000 (300 MHz ^1H; 121 MHz ^{31}P), or a Varian Unity Inova instrument (400 MHz ^1H; 162 MHz ^{31}P). Mass spectra were acquired on a PE-Sciex API III triple quadrupole spectrometer. Gas reactions were carried out on a calibrated gas line with the solution being first degassed.

dx.doi.org/10.1021/ja108426f |*J. Am. Chem. Soc.* 2011, 133, 2571–2582

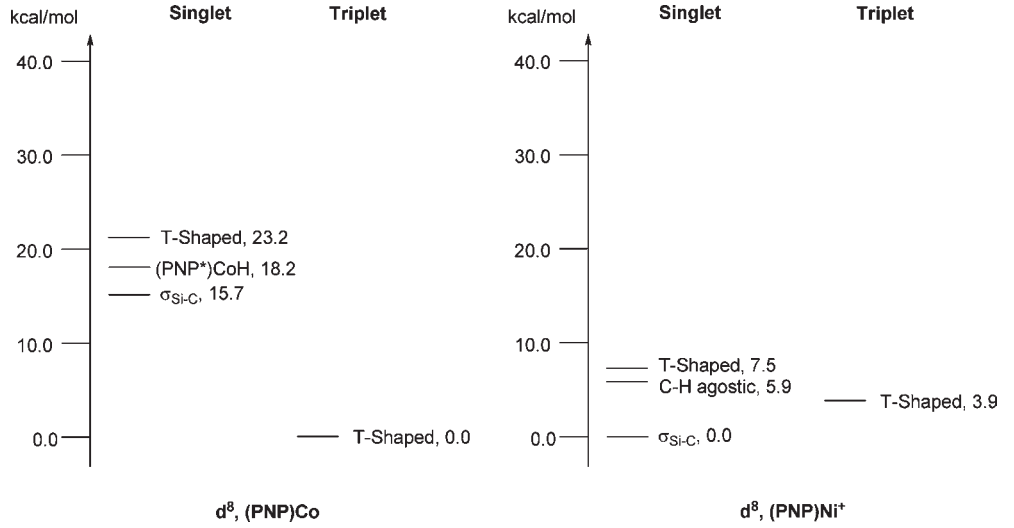

Figure 7. DFT energies of isomeric isoelectronic cobalt and nickel species in two spin states.

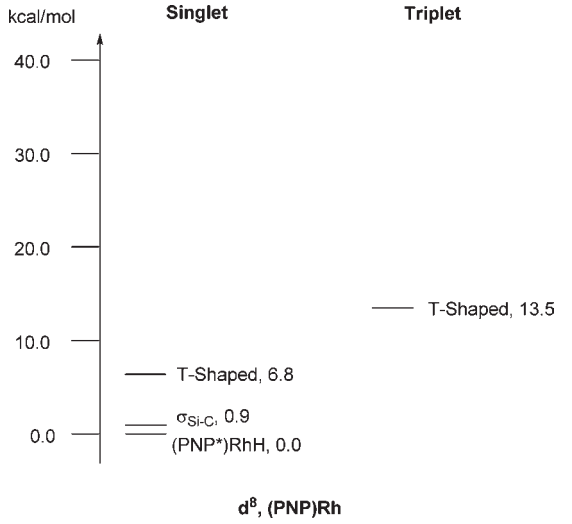

Figure 8. DFT energies of isomeric (PNP)Rh complexes, including one triplet species.

Reaction of (PNP)Ni with $[Cp^*_2Fe]B(C_6F_5)_4$. Fifteen milligrams (0.030 mmol) of (PNP)Ni was dissolved in 1 mL of d_8-THF in a J-Young NMR tube. To this solution was added 30 mg (0.030 mmol) of $Cp^*_2FeB(C_6F_5)_4$. An immediate color change was visible from pale yellow to orange. The ^1H and $^{31}P\{^1H\}$ NMR spectra were taken of the solution after 1 h. ^1H NMR (25 °C, d_8-THF): 1.43 ppm (d, J_{PH} = 13.5 Hz, ^{t}Bu, 36H), 0.40 ppm (s, SiMe, 12H), 0.27 ppm (bs, CH_2, 4H). There is no detectable signal in the $^{31}P\{^1H\}$ NMR spectrum at this time, consistent (see below) with the species identity $(PNP)Ni^+$. After 12 h the solution had polymerized and a $^{31}P\{^1H\}$ NMR spectrum was taken of the solid mass. $^{31}P\{^1H\}$ NMR (25 °C, d_8-THF): 54.6 ppm (d, J_{PP} = 198 Hz), −33.8 (d, J_{PP} = 198 Hz).

$[(^tBu_2PCH_2SiMe_2)_2N]Ni]B[3,5\text{-}(CF_3)_2C_6H_3]_4$. A solution of $[(^tBu_2PCH_2SiMe_2)_2N]NiCl$, 15 mg (0.030 mmol), was prepared in 3 mL of fluorobenzene. To this solution was added 30 mg (0.034 mmol) of $NaB[3,5\text{-}(CF_3)_2C_6H_3]_4$. The solution changed color from red to orange within 12 h. The solvent was stripped to dryness, and pentane was added. $(PNP)NiBAr^F{}_4$ oiled out in pentane and was separated by pipet. This oil was then dissolved in CD_2Cl_2, and NMR spectra were recorded. This was then stripped to dryness and dissolved in minimal dichloromethane. This solution was then layered with pentane and slow diffusion over 2 days produced crystals for X-ray diffraction studies. ^1H NMR (25 °C, CD_2Cl_2): 7.73 ppm (s, ArH, 8H), 7.57 ppm (s, ArH, 4H), 1.50 ppm (d, J_{PH} = 10.8 Hz, ^{t}Bu, 36H), 0.43 ppm (s, SiMe, 12H), −0.22 ppm (vbs, CH_2, 4H). $^{31}P\{^1H\}$ NMR (25 °C, CD_2Cl_2): no signal. ^{19}F NMR (25 °C, CD_2Cl_2): −63.1 ppm (s). $^{31}P\{^1H\}$ NMR (−55 °C, CD_2Cl_2): 102.5 ppm (d, J_{PH} = 35 Hz), 41.3 ppm (d, J_{PH} = 41 Hz). This reaction, carried out in CH_2Cl_2 over 30 min, gave an isolated yield of 83%.

$[(^tBu_2PCH_2SiMe_2)_2N](CO)]B[3,5\text{-}(CF_3)_2C_6H_3]_4$. A solution of $[(^tBu_2PCH_2SiMe_2)_2N]NiCl$ 15 mg (0.030 mmol) in 3 mL of fluorobenzene was prepared. To this solution was added 30 mg (0.034 mmol) of $NaB[3,5\text{-}(CF_3)_2C_6H_3]_4$. An atmosphere of CO was placed over the solution. The solution changed color from red to yellow within 12 h. The solvent was stripped to dryness, and CD_2Cl_2 was added for NMR analysis. This solution was then placed in a solution IR cell for IR analysis. ^1H NMR (25 °C, CD_2Cl_2): 7.74 ppm (s, ArH, 8H), 7.58 ppm (s, ArH, 4H), 1.43 ppm (t, J_{PH} = 7.6 Hz, ^{t}Bu, 36H), 1.27 ppm (t, J_{PH} = 6 Hz, CH_2, 4H), 0.28 ppm (s, SiMe, 12H). $^{31}P\{^1H\}$ NMR (25 °C, CD_2Cl_2): 90.2 ppm (s). ^{19}F NMR (25 °C, CD_2Cl_2): −63.2 ppm (s). IR (Dichloromethane): 2044 cm^{-1}. This reaction, repeated using isolated $[(^tBu_2PCH_2SiMe_2)_2N]Ni]B[3,5\text{-}(CF_3)_2C_6H_3]_4$ in CH_2Cl_2, gave an isolated yield of 90%.

$[(^tBu_2PCH_2SiMe_2)_2N]NiF$. Fifteen mg (0.028 mmol) of (PNP)NiCl was dissolved in 10 mL THF in a Schlenk flask. To this solution were added 12.6 mg (0.084 mmol) of anhydrous Me_4NF and 42.6 mg (0.28 mmol) of CsF, and this was stirred for 12 h. The solution color changed from red to a golden yellow during this time. The solution was filtered, the solvent was stripped, and the resulting solid was dissolved in C_6D_6 for NMR spectral analysis. Subsequently dissolving the solid in minimal toluene, then slowly removing the toluene under vacuum resulted in crystal formation. ^1H NMR (25 °C, C_6D_6): 1.47 ppm (t, J_{PH} = 7.5 Hz, ^{t}Bu,36H,), 0.38 ppm (t, J_{PH} = 4.8 Hz, CH_2, 4H), 0.25 (s, SiMe, 12H). $^{31}P\{^1H\}$ NMR (25 °C, C_6D_6): 34.2 ppm (d, J_{FP} = 28.3 Hz). ^{19}F NMR (25 °C, C_6D_6): −160.8 ppm (t, J_{PF} = 27.6 Hz).

$[(^tBu_2PCH_2SiMe_2NSiMe_2OTf)]Ni(CH_2P^tBu_2)]$. *1. From (PNP) Ni + AgOTf.* To a solution of 15 mg (0.030 mmol) of $[(^tBu_2PCH_2SiMe_2)_2N]Ni$ in 1 mL of C_6D_6 was added 8 mg (0.031 mmol) of AgOTf in a vial at 25 °C. The solution darkened, and a black precipitate formed after 30 s. The solution was filtered, and the filtrate was orange (distinctly different from the pale yellow of the starting material). After 48 h the solution was stripped to dryness, and minimal

dx.doi.org/10.1021/ja108426f |J. Am. Chem. Soc. 2011, 133, 2571–2582

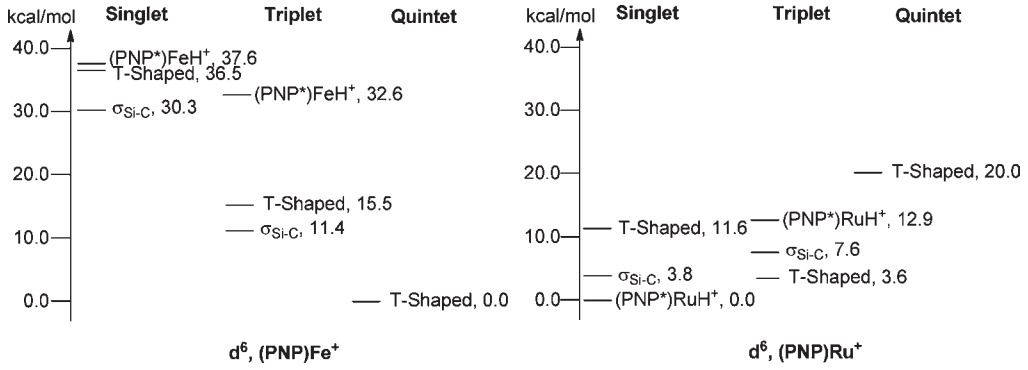

Figure 9. DFT energies of isomeric, isoelectronic Fe vs Ru PNP complexes in three spin states.

toluene was added. Toluene was slowly pumped off at 25 °C. Small crystals formed suitable for X-ray diffraction studies.

2. From (PNP)Ni + [FeCp$_2$]OTf.* To a solution of 15 mg (0.030 mmol) of [(^{t}Bu$_2$PCH$_2$SiMe$_2$)$_2$N]Ni in 0.5 mL of C_6D_6 was added 11 mg (0.033 mmol) of [FeCp*$_2$]OTf (1:1) in a J-Young NMR tube at 25 °C. NMR spectra were taken at various time increments. These spectra were similar to those found with AgOTf. The equilibrium ratio of 1:9 between isomers **A** and **B** was reached at 48 h. Also detected was the signal at 3.9 ppm of Cp*$_2$Fe.

3. From (PNP)NiF + Me$_3$SiOTf. To a solution of 15 mg (0.029 mmol) of [(^{t}Bu$_2$PCH$_2$SiMe$_2$)$_2$N]NiF in 0.5 mL of C_6D_6 was added 3-fold excess of Me$_3$SiOTf in a J-Young NMR tube at 25 °C. The solution went from golden brown to orange over 48 h. The spectra at this time were similar to those of the 1:9 equilibrium ratio between isomers **A** and **B**. Isomer **A**: ^{1}H NMR (25 °C, C_6D_6): 1.13 ppm (d, J_{PH} = 14.7 Hz, ^{t}Bu, 18H), 1.09 ppm (d, J_{PH} = 10 Hz, ^{t}Bu, 18H), 0.64 ppm (s,SiMe, 6H), 0.54 ppm (s,SiMe, 6H), 0.41 ppm (d, J_{PH} = 6 Hz,CH$_2$, 2H), 0.31 ppm (d, J_{PH} = 9.6 Hz,CH$_2$, 2H). ^{31}P{^{1}H} NMR (25 °C, C_6D_6): 61.6 ppm (d, J_{PP} = 27 Hz), 5.3 ppm (d, J_{PP} = 27 Hz). Isomer **B**: ^{1}H NMR (25 °C, C_6D_6): 1.2 ppm (d, J_{PH} = 14.7 Hz, ^{t}Bu, 18H), 1.1 ppm (d, J_{PH} = 13 Hz, ^{t}Bu, 18H), 0.69 ppm (s,SiMe, 6H), 0.48 ppm (d, J_{PH} = 12 Hz,CH$_2$, 2H), 0.43 ppm (s,SiMe, 6H), −0.5 ppm (d, J_{PH} = 5 Hz,CH$_2$, 2H). ^{31}P{^{1}H} NMR (25 °C, C_6D_6): 58.4 ppm (d, J_{PP} = 213 Hz), −34.0 ppm (d, J_{PP} = 213 Hz).

[(^{t}Bu$_2$PCH$_2$SiMe$_2$)$_2$NH]NiH(OTf). A solution of (^{t}Bu$_2$PCH$_2$-SiMe$_2$NSiMe$_2$OTf)]Ni(CH$_2$P^{t}Bu$_2$) (15 mg, 0.023 mmol) in 0.5 mL of C_6D_6 was freeze−pump−thaw degassed. To this J-Young NMR tube was added 760 mmHg of H_2 on a vacuum line. After 1 week of end-over-end agitation, the solution had changed color from orange to yellow and a colorless precipitate had formed. The solution was filtered, and the solid was dissolved in deuterated THF for NMR spectral analysis. This solution was then layered with pentane to allow for slow diffusion. From this solution, colorless needles were grown for X-ray diffraction analysis. ^{1}H NMR (25 °C, d_8-THF) 2.80 ppm (s, NH, 1H), 1.37 ppm (t, J_{PH} = 7.5 Hz, ^{t}Bu, 18H), 1.28 ppm (t, J_{PH} = 7.2 Hz, ^{t}Bu, 18H), 0.89 ppm (t, J_{PH} = 6.3 Hz, CH$_2$, 2H), 0.59 ppm (s,SiMe, 6H), 0.34 ppm (s,SiMe, 6H), −22.37 ppm (t, J_{PH} = 68.4 Hz, NiH, 1H). The second CH$_2$ peak is obscured by the ^{t}Bu peaks. ^{31}P{^{1}H} NMR (25 °C, d_8-THF): 62.9 ppm.

[(^{t}Bu$_2$PCH$_2$SiMe$_2$)$_2$NH]NiH(BAr$^F_4$). A solution of 20 mg (0.039 mmol) of (PNP)NiCl and 35 mg (0.039 mmol) of NaB[3,5-(CF$_3$)$_2$-C$_6$H$_3$]$_4$ in 0.5 mL of CD_2Cl_2 was agitated end-over-end for 1 h to form [(PNP)Ni]BAr$^F_4$. The solution was freeze−pump−thaw degassed, and 760 mmHg of H_2 was added on a vacuum line. In time of mixing the solution had changed color from red to yellow. NMR analysis showed complete conversion into (PN(H)P)NiH(BAr$^F_4$). ^{1}H NMR (25 °C, CD_2Cl_2): 7.76 ppm (br.s, Ar-*o*, 8 H), 7.59 ppm (br.s, Ar-*p*, 4 H), 1.33 ppm (t, J_{PH} = 7.0 Hz, ^{t}Bu, 18H), 1.32 ppm (t, J_{PH} = 7.0 Hz, ^{t}Bu, 18H), 1.23−1.26 ppm (m, CH$_2$, 4H), 0.48 ppm (s, SiMe, 6H), 0.39 ppm (s, SiMe, 6H), −22.06 ppm (t, J_{PH} = 66.1 Hz, Ni−H, 1H). N−H proton was not located. ^{31}P{^{1}H} NMR (25 °C, CD_2Cl): 63.2 ppm. ^{19}F NMR (25 °C, CD_2Cl_2): −63.2 ppm (s).

[(^{t}Bu$_2$PCH$_2$SiMe$_2$)$_2$N]NiH. *1. From [(PN(H)P)NiH]OTf and Et$_3$N in D$_8$THF.* Fifteen milligrams (0.023 mmol) of [(^{t}Bu$_2$PCH$_2$SiMe$_2$)$_2$ NH]NiH(OTf) was dissolved in 0.5 mL of deuterated THF. To this solution was added a 10-fold excess (3.2 μL) of Et$_3$N. The NMR of the resulting yellow solution showed 90% conversion to (PNP)NiH. ^{1}H NMR (25 °C, d_8-THF): 1.30 ppm (t, J_{PH} = 6.3 Hz, ^{t}Bu, 36H), 0.95 ppm (t, J_{PH} = 6.6 Hz, CH$_2$, 4H), 0.61 ppm (s, SiMe, 12H), −21.30 ppm (t, J_{PH} = 66 Hz, NiH, 1H). ^{31}P{^{1}H} NMR (25 °C, d_8-THF): 73.2 ppm. CI-MS (THF solution, *m/z*): obsd 507.2548 [M]$^+$ $C_{22}H_{53}NNiP_2Si_2$; theory 507.2540.

2. From [(PN(H)P)Ni(H)]BAr$^F_4$ and LiN^{i}Pr$_2$ in THF. A solution of (PN(H)P)NiH(BAr$^F_4$) in CD_2Cl_2 obtained from 20 mg (0.039 mmol) of (PNP)NiCl, 35 mg of NaB[3,5-(CF$_3$)$_2$C$_6$H$_3$]$_4$, and 1 atm H_2 (see above) was dried in vacuum and dissolved in 3 mL of THF. Next, 4.2 mg (0.039 mmol) of LiN^{i}Pr$_2$ was added. After 10 min of stirring, all volatiles were removed in vacuum. The residue was extracted with 2 × 10 mL of pentane and filtered through a glass filter. Pentane was removed in a vacuum, and the yellow solid was dissolved in C_6D_6 for NMR analysis. ^{1}H NMR (25 °C, C_6D_6): 1.23 ppm (t, J_{PH} = 6.4 Hz, ^{t}Bu, 36H), 0.82 ppm (t, J_{PH} = 4.8 Hz, CH$_2$, 4H), 0.40 ppm (s, SiMe, 12H), −21.19 ppm (t, J_{PH} = 68 Hz, NiH, 1H). ^{31}P{^{1}H} NMR (25 °C, C_6D_6): 73.8 ppm.

3. From (PNP)NiCl + NaBH$_4$. Fifteen milligrams (0.030 mmol) of (PNP)NiCl was dissolved in 1 mL of THF in a J-Young NMR tube. To this solution was added a slight excess 1.5 mg (0.039 mmol) of NaBH$_4$. The ^{1}H and ^{31}P{^{1}H} NMR were recorded after 12 h. These spectra show production of known (PNP)Ni and (PNP)NiH (apparent from hydride triplet at −21.3 ppm). Also a ^{t}Bu doublet in the ^{1}H NMR along with a broad signal in the ^{31}P{^{1}H} is consistent with production of a small amount of metal-free phosphine-borane adduct; this side reaction correlates with the appearance of a black solid, attributed to nickel metal.

Reaction of (PNP)NiF with BF$_3$·Et$_2$O, forming [(^{t}Bu$_2$PCH$_2$-SiMe$_2$NSiMe$_2$F)]Ni(CH$_2$P^{t}Bu$_2$)] and its BF$_3$ adduct. *1. With a catalytic amount of BF$_3$·Et$_2$O.* Fifteen milligrams (0.030 mmol) of (PNP)NiF was dissolved in 1 mL of C_6D_6 in a J-Young NMR tube. To this solution was added 1 μL of BF$_3$·Et$_2$O (0.01 mmol, ∼30 mol %). The solution color changed from golden brown to orange red in 5 min. At 30 min the ^{1}H and ^{31}P{^{1}H} NMR of the solution showed two products (see NMR below). This solution was stripped to dryness and dissolved in THF for mass spectral analysis. The solution was then stripped to dryness again and redissolved in C_6D_6 for analysis by ^{1}H and ^{31}P{^{1}H} NMR, to establish product lifetime. [(^{t}Bu$_2$PCH$_2$SiMe$_2$N-SiMe$_2$F)]Ni(CH$_2$P^{t}Bu$_2$)] ^{1}H NMR (25 °C, C_6D_6): 1.34 ppm (d, J_{PH} = 14.2 Hz, ^{t}Bu, 18H), 1.21 ppm (d, J_{PH} = 12.3 Hz, ^{t}Bu, 18H), 0.45 ppm (d, J_{FH} = 6 Hz, SiMe, 6H), 0.41 ppm (s, SiMe, 6H), −0.47 ppm

dx.doi.org/10.1021/ja108426f |*J. Am. Chem. Soc.* 2011, 133, 2571–2582

(d, J_{PH} = 4.2 Hz, CH_2, 2H); the second CH_2 is not positively identified due to overlap with silyl methyl groups. $^{31}P\{^1H\}$ NMR (25 °C, C_6D_6): 62.3 ppm (dd, J_{PP} = 232, J_{PF} = 6.2, Hz), −24.3 ppm (dd, J_{PP} = 232, J_{PF} = 30.8, Hz). $^{19}F\{^1H\}$ NMR (25 °C, C_6D_6): −116.3 ppm (m, J_{PF} = 30.5 Hz, J_{HF} 6 Hz). ESI-MS (m/z): 525.29 $[M + H]^+$, 450.26 $[M]^+$. ^1H NMR of BF_3 adduct (25 °C, C_6D_6): 1.29 ppm (d, J_{PH} = 14.5 Hz, ^{t}Bu, 18H), 1.19 ppm (d, J_{PH} = 12.8 Hz, ^{t}Bu, 18H), 0.75 ppm (d, J_{FH} = 5 Hz, SiMe, 6H), 0.59 ppm (s,SiMe, 6H), −0.07 ppm (d, J_{PH} = 6 Hz, CH_2, 2H) the second CH_2 is not positively identified. $^{31}P\{^1H\}$ NMR of BF_3 adduct (25 °C, C_6D_6): 45.1 ppm (d, J_{PP} = 190 Hz), −48.7 ppm (d, J_{PP} = 191 Hz). $^{19}F\{^1H\}$ NMR of BF_3 adduct (25 °C, C_6D_6): −125.1 ppm (q, J_{FB} = 30 Hz), −125.6 ppm (s).

2. With equimolar $BF_3 \cdot Et_2O$. The experiment was carried out with 3 μL $BF_3 \cdot Et_2O$ (1:1) ratio, to establish the identity of the minor product above as a BF_3 adduct. After 30 min ^1H and $^{31}P\{^1H\}$ NMR were recorded, which showed complete conversion to the BF_3 adduct produced in smaller mole fraction above. Crystals were grown by slow evaporation of solvent over several days and were identified by X-ray diffraction as the product of hydrolysis of the BF_3, from released HF.

Reaction with DBU and Its Impact on Hydrogenation Reactivity. A solution of 20 mg (0.039 mmol) of (PNP)NiCl and 35 mg (0.039 mmol) of $NaB[3,5\text{-}(CF_3)_2C_6H_3]_4$ in 0.5 mL of d_8-THF was stirred for 24 h. According to both ^{31}P and ^1H NMR there is no reaction. THF was removed in vacuo, and the residue was redissolved in 0.5 mL of CD_2Cl_2. ^1H and ^{31}P NMR showed partial conversion (∼50%) into $(PNP)Ni[3,5\text{-}(CF_3)_2C_6H_3]_4$ after 24 h with vigorous stirring. Next, 0.0043 mL (4.4 mg, 0.029 mmol) of DBU (1,8-diazabicyclo[5.4.0] undec-7-ene) was added via syringe. The solution was freeze−pump−thaw degassed, and 760 mmHg of H_2 was added on a vacuum line. ^{31}P NMR of the solution in 10 min showed formation of the *kinetic* product of attack of BDU at silicon. $^{31}P\{^1H\}$ NMR (25 °C, CD_2Cl_2): 59.5 and 3.1 ppm (both d, J = 30 Hz). In 4 days one could see formation of the second product, the DBU attack product on silicon with the two P mutually *trans*. $^{31}P\{^1H\}$ NMR (25 °C, CD_2Cl_2): 55.0 and −38.2 ppm (both d, J = 205 Hz) together with some amount of the deprotonation product of $(PN(H)P)NiH^+$, (PNP)NiH.

■ ASSOCIATED CONTENT

Supporting Information. Full computational details along with crystallographic details in CIF format. This material is available free of charge via the Internet at http://pubs.acs.org.

■ AUTHOR INFORMATION

Corresponding Author
caulton@indiana.edu

■ ACKNOWLEDGMENT

We thank the National Science Foundation (NSF CHE-0544829) for financial support. We thank Prof. Daniel Mindiola for gifts of several useful oxidants for this work and Dr. Michael Ingleson for useful discussion.

■ REFERENCES

(1) Fan, H.; Fullmer, B. C.; Pink, M.; Caulton, K. G. *Angew. Chem., Int. Ed.* **2008**, *47*, 9112.
(2) Fan, L.; Ozerov, O. V. *Chem. Commun.* **2005**, 4450.
(3) Ozerov, O. V.; Guo, C.; Fan, L.; Foxman, B. M. *Organometallics* **2004**, *23*, 5573.
(4) Wang, L.; Wang, Z.-X. *Org. Lett.* **2007**, *9*, 4335.
(5) Benito-Garagorri, D.; Mereiter, K.; Kirchner, K. *Eur. J. Inorg. Chem.* **2006**, 4374.
(6) Campora, J.; Palma, P.; del Rio, D.; Mar Conejo, M.; Alvarez, E. *Organometallics* **2004**, *23*, 5653.
(7) Campora, J.; Palma, P.; Del Rio, D.; Alvarez, E. *Organometallics* **2004**, *23*, 1652.
(8) van der Boom, M. E.; Liou, S.-Y.; Shimon, L. J. W.; Ben-David, Y.; Milstein, D. *Inorg. Chim. Acta* **2004**, *357*, 4015.
(9) Melaimi, M.; Thoumazet, C.; Ricard, L.; Floch, P. L. *J. Organomet. Chem.* **2004**, *689*, 2988.
(10) Gossage, R. A.; van de Kuil, L. A.; van Koten, G. *Acc. Chem. Res.* **1998**, *31*, 423.
(11) Benito-Garagorri, D.; Kirchner, K. *Acc. Chem. Res.* **2008**, *41*, 201.
(12) Boeing, C.; Francio, G.; Leitner, W. *Adv. Synth. Catal.* **2005**, *347*, 1537.
(13) Tomita, T.; Takahama, T.; Sugimoto, M.; Sakaki, S. *Organometallics* **2002**, *21*, 4138.
(14) Mecking, S. *Coord. Chem. Rev.* **2000**, *203*, 325.
(15) Cherian, A. E.; Rose, J. M.; Lobkovsky, E. B.; Coates, G. W. *J. Am. Chem. Soc.* **2005**, *127*, 13770.
(16) Williams, B. S.; Leatherman, M. D.; White, P. S.; Brookhart, M. *J. Am. Chem. Soc.* **2005**, *127*, 5132.
(17) Malinoski, J. M.; Brookhart, M. *Organometallics* **2003**, *22*, 5324.
(18) Leatherman, M. D.; Svejda, S. A.; Johnson, L. K.; Brookhart, M. *J. Am. Chem. Soc.* **2003**, *125*, 3068.
(19) Johnson, L. K.; Killian, C. M.; Brookhart, M. *J. Am. Chem. Soc.* **1995**, *117*, 6414.
(20) Del Zotto, A.; Zangrando, E.; Baratta, W.; Felluga, A.; Martinuzzi, P.; Rigo, P. *Eur. J. Inorg. Chem.* **2005**, 4707.
(21) Liang, L.-C.; Chien, P.-S.; Lin, J.-M.; Huang, M.-H.; Huang, Y.-L.; Liao, J.-H. *Organometallics* **2006**, *25*, 1399.
(22) Horton, A. D.; Orpen, A. G. *Organometallics* **1991**, *10*, 3910.
(23) Nueckel, S.; Burger, P. *Organometallics* **2001**, *20*, 4345.
(24) DeMott, J. C.; Basuli, F.; Kilgore, U. J.; Foxman, B. M.; Huffman, J. C.; Ozerov, O. V.; Mindiola, D. J. *Inorg. Chem.* **2007**, *46*, 6271.
(25) Kazi, A. B.; Jones, G. D.; Vicic, D. A. *Organometallics* **2005**, *24*, 6051.
(26) Gomez-Benitez, V.; Baldovino-Pantaleon, O.; Herrera-Alvarez, C.; Toscano, R. A.; Morales-Morales, D. *Tetrahedron Lett.* **2006**, *47*, 5059.
(27) Pugh, D.; Boyle, A.; Danopoulos, A. A. *Dalton Trans.* **2008**, 1087.
(28) Fossey, J. S.; Richards, C. J. *J. Organomet. Chem.* **2004**, *689*, 3056.
(29) Pandarus, V.; Zargarian, D. *Organometallics* **2007**, *26*, 4321.
(30) Liang, L.-C.; Chien, P.-S.; Huang, Y.-L. *J. Am. Chem. Soc.* **2006**, *128*, 15562.
(31) Castonguay, A.; Sui-Seng, C.; Zargarian, D.; Beauchamp, A. L. *Organometallics* **2006**, *25*, 602.
(32) Fischbach, A.; Bazinet, P. R.; Waterman, R.; Tilley, T. D. *Organometallics* **2008**, *27*, 1135.
(33) Liang, L.-C.; Lin, J.-M.; Hung, C.-H. *Organometallics* **2003**, *22*, 3007.
(34) Jones, G. D.; Martin, J. L.; McFarland, C.; Allen, O. R.; Hall, R. E.; Haley, A. D.; Brandon, R. J.; Kanovalova, T.; Desrochers, P. J.; Pulay, P.; Vicic, D. A. *J. Am. Chem. Soc.* **2006**, *128*, 13175.
(35) Marchetti, F.; Pampaloni, G.; Zacchini, S. *Inorg. Chem.* **2008**, *47*, 365.
(36) Poverenov, E.; Gandelman, M.; Shimon, L. J. W.; Rozenberg, H.; Ben-David, Y.; Milstein, D. *Organometallics* **2005**, *24*, 1082.
(37) Marsella, J. A.; Curtis, C. J.; Bercaw, J. E.; Caulton, K. G. *J. Am. Chem. Soc.* **1980**, *102*, 7244.
(38) Ingleson, M. J.; Fullmer, B. C.; Buschhorn, D. T.; Fan, H.; Pink, M.; Huffman, J. C.; Caulton, K. G. *Inorg. Chem.* **2008**, *47*, 407.
(39) Bolton, P. D.; Clot, E.; Adams, N.; Dubberley, S. R.; Cowley, A. R.; Mountford, P. *Organometallics* **2006**, *25*, 2806.
(40) Suresh, C. H.; Baik, M.-H. *Dalton Trans.* **2005**, 2982.
(41) See Supporting Information.
(42) Perutz, R. N.; Sabo-Etienne, S. *Angew. Chem., Int. Ed.* **2007**, *46*, 2578.

(43) Jones, W. D.; Vetter, A. J.; Wick, D. D.; Northcutt, T. O. *ACS Symp. Ser.* **2004**, *885*, 56.
(44) Crabtree, R. H. *Angew. Chem.* **1993**, *105*, 828.
(45) Crabtree, R. H. *J. Organomet. Chem.* **2004**, *689*, 4083.
(46) Van der Heijden, H.; Schaverien, C. J.; Orpen, A. G. *Organometallics* **1989**, *8*, 255.
(47) Alelyunas, Y. W.; Baenziger, N. C.; Bradley, P. K.; Jordan, R. F. *Organometallics* **1994**, *13*, 148.
(48) Perrin, L.; Maron, L.; Eisenstein, O.; Lappert, M. F. *New J. Chem.* **2003**, *27*, 121.
(49) Brady, E. D.; Clark, D. L.; Gordon, J. C.; Hay, P. J.; Keogh, D. W.; Poli, R.; Scott, B. L.; Watkin, J. G. *Inorg. Chem.* **2003**, *42*, 6682.
(50) Baidya, M.; Mayr, H. *Chem. Commun.* **2008**, 1792.
(51) Ingleson, M. J.; Pink, M.; Fan, H.; Caulton, K. G. *J. Am. Chem. Soc.* **2008**, *130*, 4262.
(52) Walstrom, A.; Pink, M.; Tsvetkov, N. P.; Fan, H.; Ingleson, M.; Caulton, K. G. *J. Am. Chem. Soc.* **2005**, *127*, 16780.